BARC/2009/E/023

CHARACTERIZATION OF ELECTRON BEAM DEPOSITED THIN FILMS OF HfO_2 AND BINARY THIN FILMS OF (HfO_2:SiO_2) BY XRD AND EXAFS MEASUREMENTS

by

N.C. Das, N.K. Sahoo, D. Bhattacharyya,
S. Thakur and N.M. Kamble
Spectroscopy Division, BARC
and
D. Nanda
Coolant System Laboratory, Raja Ramanna Centre
for Advanced Technology, Indore

and
S. Hazra and J.K. Bal
Surface Physics Division, Saha Institute of Nuclear
Physics, Kolkata
and
J.F. Lee, Y.L. Tai and C.A. Hsieh
National Synchrotron Radiation Research Centre,
Hsinchu, Taiwan, R.O.C.

2009

BARC/2009/E/023

BARC/2009/E/023

GOVERNMENT OF INDIA
ATOMIC ENERGY COMMISSION

CHARACTERIZATION OF ELECTRON BEAM DEPOSITED THIN FILMS OF HfO_2 AND BINARY THIN FILMS OF (HfO_2:SiO_2) BY XRD AND EXAFS MEASUREMENTS

by

N.C. Das, N.K. Sahoo, D. Bhattacharyya, S. Thakur and N.M. Kamble
Spectroscopy Division, BARC
and
D. Nanda
Coolant System Laboratory, Raja Ramanna Centre for Advanced Technology, Indore
and
S. Hazra and J.K. Bal
Surface Physics Division, Saha Institute of Nuclear Physics, Kolkata
and
J.F. Lee, Y.L. Tai and C.A. Hsieh
National Synchrotron Radiation Research Centre, Hsinchu, Taiwan, R.O.C.

BHABHA ATOMIC RESEARCH CENTRE
MUMBAI, INDIA
2009

BIBLIOGRAPHIC DESCRIPTION SHEET FOR TECHNICAL REPORT
(as per IS : 9400 - 1980)

01	*Security classification :*	Unclassified
02	*Distribution :*	External
03	*Report status :*	New
04	*Series :*	BARC External
05	*Report type :*	Technical Report
06	*Report No. :*	BARC/2009/E/023
07	*Part No. or Volume No. :*	
08	*Contract No. :*	
10	*Title and subtitle :*	Characterization of electron beam deposited thin films of HfO_2 and binary thin films of (HfO_2:SiO_2) by XRD and EXAFS measurements
11	*Collation :*	44 p., 16 figs., 1 tab.
13	*Project No. :*	
20	*Personal author(s) :*	1) N.C. Das; N.K. Sahoo; D. Bhattacharyya; S. Thakur; N.M. Kamble 2) D. Nanda 3) S. Hazra; J.K. Bal 4) J.F. Lee; Y.L. Tai; C.A. Hsieh
21	*Affiliation of author(s) :*	1) Spectroscopy Division, Bhabha Atomic Research Centre, Mumbai 2) Coolant System Laboratory, Raja Ramanna Centre for Advanced Technology, Indore 3) Surface Physics Division, Saha Institute of Nuclear Physics, Kolkata 4) National Synchrotron Radiation Research Center, Hsinchu, Taiwan, R.O.C.
22	Corporate author(s) :	Bhabha Atomic Research Centre, Mumbai-400 085
23	*Originating unit :*	Spectroscopy Division, BARC, Mumbai
24	*Sponsor(s) Name :* *Type :*	Department of Atomic Energy Government

Contd...

30	*Date of submission :*	September 2009
31	*Publication/Issue date :*	October 2009
40	*Publisher/Distributor :*	Associate Director, Knowledge Management Group and Head, Scientific Information Resource Division, Bhabha Atomic Research Centre, Mumbai
42	*Form of distribution :*	Hard copy
50	*Language of text :*	English
51	*Language of summary :*	English, Hindi
52	*No. of references :*	54 refs.
53	*Gives data on :*	

60 *Abstract :* In this report, we have discussed the microstructure and the local structure of composite thin films having varying hafnia and silica compositions and prepared by reactive electron beam evaporation. XRD and EXAFS studies have confirmed that the pure hafnium oxide thin film has crystalline microstructure whereas the films with finite hafnia and silica composition are amorphous. The result of EXAFS analysis has shown that the bond lengths as well as coordination numbers around hafnium atom change with the variation of hafnia and silica compositions in the thin film. Finally, change of bond lengths has been correlated with change of refractive index and band gap of the composite thin films.

70	*Keywords/Descriptors :*	THIN FILMS; HAFNIUM OXIDES; ELECTRON BEAMS; X-RAY DIFFRACTION; REFRACTIVE INDEX; GRADED BAND GAPS; CHEMICAL VAPOR DEPOSITION; SILICON
71	*INIS Subject Category :*	S75
99	*Supplementary elements :*	

सारांश

प्रस्तुत रिपोर्ट में प्रतिक्रियाशील इलेक्ट्रान किरण वाष्पीकरण द्वारा निर्मित मिश्रित तनु फिल्मों की सुक्ष्म व स्थानीय संरचना की विवेचना की गयी है। XRD व EXAFS द्वारा किये गये अध्यमन में यह पाया गया है कि शुध्द हाफनियम ऑक्साइड तनु फिल्में क्रिस्टलीय प्रवृति की है जबकि हाफनिया-सिलिका मिश्रित तनु फिल्मों की संरचना बेढब है। EXAFS द्वारा प्राप्त परिणामों से ये भी दर्शाया गया है कि हाफनियम परमाणु के आस-पास की बान्ड-लम्बाई और कॅर्डिनेशन संख्या तनु फिल्मों में उपस्थित हाफनियम व सिलिका की मात्रा के अनुसार परिवर्तित होती हैं। बान्ड की लम्बाई में होने वाले परिवर्तन का सम्बन्ध इन मिश्रित तनु फिल्मों के अपवर्तनांक और बैन्ड-अंतराल के साथ स्थापित किया गया है।

Characterization of electron beam deposited thin films of HfO_2 and binary thin films of (HfO_2:SiO_2) by XRD and EXAFS measurements

N. C. Das[a] , N. K. Sahoo[a], D. Bhattacharyya[a], S. Thakur[a], N. M. Kamble[a], D. Nanda[b], S. Hazra[c], J. K. Bal[c], J. F. Lee[d], Y. L. Tai[d], C. A. Hsieh[d]

Abstract

In this report, we have discussed the microstructure and the local structure of composite thin films having varying hafnia and silica compositions and prepared by reactive electron beam evaporation. XRD and EXAFS studies have confirmed that the pure hafnium oxide thin film has crystalline microstructure whereas the films with finite hafnia and silica composition are amorphous. The result of EXAFS analysis has shown that the bond lengths as well as coordination numbers around hafnium atom change with the variation of hafnia and silica compositions in the thin film. Finally, change of bond lengths has been correlated with change of refractive index and band gap of the composite thin films.

---

[a]Spectroscopy Division, Bhabha Atomic Research Centre, Mumbai

[b]Coolant System Laboratory, Raja Rmanna Centre for Advanced Technology, Indore

[c]Surface Physics Division, Saha Institute of Nuclear Physics, Kolkata

[d]National Synchrotron Radiation Research Center, Hsinchu,Taiwan, R. O. C.

Characterization of electron beam deposited thin films of HfO_2 and binary thin films of (HfO_2:SiO_2) by XRD and EXAFS measurements

1. Introduction

Hafnium oxide (HfO_2) has been extensively studied as a promising high-*K* dielectric [1,2] to replace conventional silicon oxide (SiO_2) gate dielectric in the sub-0.1μm complementary metal-oxide semiconductor (CMOS) technology due to its high melting point, thermal and chemical stability, relatively high refractive index and its superior thermodynamic stability in contact with silicon. It has high dielectric constant (> 20), wide band gap of the order of 6 eV and 1.5 eV band offsets with silicon. During studying hafnium oxide as an alternate gate dielectric, it has been deposited on silicon substrate by various deposition methods, such as, atomic layer deposition [3,4,5,6], chemical vapour deposition [7,8,9], sol-gel process [10], reactive sputtering [11], pulsed deposition [12,13,14,15,16,17], etc.

Thin films of HfO_2 deposited by the above mentioned methods have been characterized generally by performing some of the following measurements. The thickness and refractive index of the films have been measured by ellipsometry. The surface morphology of the films has been measured by atomic force microscopy (AFM) and scanning electron microscopy (SEM) whereas the interfacial properties have been evaluated by transmission electron microscopy (TEM). X-ray photoelectron spectroscopy (XPS) has been used for the estimation of the chemical composition of the films. The crystal structure and amorphousness of the films have been measured directly by X-ray diffraction (XRD). The knowledge of the local structure around Hf atom, such as bond

length or the number of nearest neighbors as well as the crystalline and amorphous phases for the thin films have been obtained by extended x-ray absorption fine structure (EXAFS) measurements [5,6,11,14,16,17,18] around L_3-edge of hafnium.

As discussed in reference [6], amorphousness is highly desirable in high-*K* gate oxide materials for their application in metal oxide semiconductor devices since the lack of grain boundaries in amorphous materials prevents the leakage current as well as fluctuations in the carrier concentration through local charge trapping. It also provides compositional stability during the fabrication process of metal oxide semiconductor devices. The importance of the local atomic structure information lies in the fact that the microscopic properties, such as the dielectric response, the charge distribution, and band gap, significantly depend on the local atomic distribution. We have, therefore, summarized the XRD and EXAFS studies of HfO_2-thin films deposited on silicon substrate as follows.

The as-deposited films developed through atomic layer deposition [3,5,6], photo induced chemical vapor deposition [7,9] and sputtering technique [18] and films developed around 500^0C through sol-gel preparation [10] have shown amorphous phases. Pure monoclinic phase, however, have been observed in films when developed by sol-gel process at temperature above 500^0C. Monoclinic phases have also been observed in films when subjected to post deposition thermal annealing [3,18,6]. It may be mentioned that films subjected to post deposition rapid thermal annealing [3] as well as films grown by chemical vapor deposition [8] at 450^0C have become polycrystalline. Finally, the transformation of orthorhombic to tetragonal to monoclinic phases in HfO_2 films during

post deposition annealing [5] and tetragonal to monoclinic phase transformation upon increase in the substrate temperature [17] have also been observed.

One important outcome of the EXAFS studies on hafnium oxide [6] is that the measured first-shell intensities in the two spectra of amorphous hafnium oxide (*a*-HfO_2) and crystalline hafnium oxide (*c*-HfO_2) films are almost identical which implies that the number of near neighbors and the disorder along the Hf-O bond direction in *a*-HfO_2 are similar to those in *c*-HfO_2. Therefore, the local structure of the *a*-HfO_2 film has been analyzed on the basis of monoclinic local structure as XRD studies has confirmed the monoclinic phase in *c*-HfO_2. The analysis has suggested that the local structure ordering in *a*-HfO_2 is similar to that of monoclinic HfO_2 with seven near neighbors along the Hf-O bond direction.

Because of its high refractive index and transparency over a wide spectral range extending from deep ultraviolet to the mid-infrared regions [19,21,24,34,36] and high laser-induced damage threshold [25,27,28,32,37], hafnium oxide has extensively been used in the development of thin film optical coatings and multi-layered optical components for use in the UV and infrared regions. These include anti-reflecting coating [21,22,38,40], high reflectivity mirror [35], phase unifying mirror [41], heat mirror [23], dichroic mirror [39], polariser [20], long pass UV-edge filter [29,30], UV-Raman edge filter [26], etc. In course of laser damage studies and development of multilayered optical thin film systems, hafnium oxide has been deposited mostly on silica substrates by various techniques. These include, conventional electron beam evaporation [19,20,21,22,23,24], ion assisted electron beam evaporation [25,26,27,28,29,30,31],

reactive electron beam evaporation [32,33] and various types of sputtering [25,34,35,36,37,38,39].

The optical properties of hafnium oxide thin films have been found to be dependent on various deposition techniques mentioned above and process parameters during the deposition. While characterizing the optical properties of the deposited thin films of hafnium oxide, the optical constants (n, k) of the films have been computed from the transmission, reflection and thickness measurements. It has been reported that the films coated by ion-assisted electron beam evaporation [30] have higher values for n, as compared to that of the films deposited by conventional electron beam evaporation. Although the values of k for the films deposited by both the techniques are quite small, the ion assisted deposited film has higher value for k as compared to that of the film deposited by conventional electron beam evaporation. As discussed in reference [35], the films developed by ion beam sputtering have higher values for n and lower values for k in the deep UV region as compared to those of the films developed by plasma ion assisted deposition. When comparing the optical properties of thin films deposited by conventional electron beam evaporation [23], r.f. magnetron sputtering [36] and reactive magnetron sputtering [34,38], the highest values of n and the lowest values k of have been reported in the deep UV to near infrared region corresponding to the film deposited by reactive magnetron sputtering [34].

Recently, comprehensive studies have been carried out on the optical properties, surface morphology, film homogeneity and crystal phases of hafnium oxide films deposited on silica or quartz substrate. As usual, spectroscopic ellipsometry and spectrophotometry have been applied for the measurements of refractive index, extinction

coefficient, transmission and reflectivity in the deep UV to near infrared region of the spectrum. Surface roughness and film homogeneity have been measured by atomic force microscopy (AFM) and scanning electron microscopy (SEM) respectively, whereas, x-ray diffraction (XRD) have been applied for crystal phase studies of the thin films of hafnium oxide. It has been reported that the as-deposited films produced by r.f. magnetron sputtering [36] and reactive magnetron sputtering[38] are characterized by amorphous phase, high transmissibility in the deep UV to near infrared wavelength region and small values of surface roughness. Annealing the film to high temperature has resulted in substantial reduction of the optical transmission and crystal phase transition to monoclinic phase [38]. Thin films of hafnium oxide deposited by plasma ion assisted electron beam evaporation [31] have been characterized for three samples corresponding to low, medium and high values of plasma ion momentum transfer. It has been reported that the films corresponding to low and high values of the momentum transfer have lower refractive indices and higher optical band gaps as measured at 250 nm wavelength. For both the cases, the films are characterized by inhomogeneous microstructure and monoclinic phase. On the contrary, the film corresponding to the medium value of the plasma ion momentum transfer has higher refractive index with lower optical band gap, smaller value for surface roughness, homogeneous microstructure and amorphous phase. Thus amorphous thin film of hafnium oxide having high refractive index, high transmission and minimum surface roughness has been found to be very much suitable for antireflection coating [38].

Hafnium oxide has also been used in the development of mixed composite films with low index refractory materials. Binary oxide system of (HfO_2:SiO_2) has been studied for

its suitability towards an alternate gate dielectric material. In course of this study, thin films of hafnium silicate has been deposited on silicon substrate by electron beam evaporation and sputtering [42]. High resolution transmission electron microscopy (TEM) images have shown that both as-deposited and annealed films are amorphous demonstrating the thermodynamic stability of the film with silicon. XRD studies of the thin films of (HfO_2:SiO_2) prepared by chemical solution deposition on silicon wafer [43] have been carried out for various % composition of HfO_2 and annealing temperature. It has been reported that the phase separation and crystallization of tetragonal HfO_2 was observed in the film having HfO_2 concentrations $\geq$ 50% and $\leq$ 25% when annealed at 800^0C and 1000^0C respectively. When XRD was performed on silica free HfO_2 film, crystallization of monoclinic HfO_2 was observed after annealing at 500-1200^0C. XPS studies have also been carried out on thin films of (HfO_2:SiO_2) prepared by sol-gel process [44] on silica substrate for investigating the chemical composition of the thin films as well as the nature of chemical bonds present. It has been reported that all the as-prepared samples are characterized by high carbon content which reduced to very low value after calcinations. In order to estimate the crystallization and microstructure of HfO_2 in the thin films of (HfO_2:SiO_2) on silica substrates having 70% HfO_2 and 30% SiO_2 composition and prepared by sol-gel process [45], both XRD and EXAFS experiments have been have carried out on these films subjected to various heat treatments. It has been observed that the film remains fully amorphous at least up to 900^0C, even after long heat treatment. Thermal annealing at 1000^0C for short period resulted in the crystallization of HfO_2 in the tetragonal phase. Partial transformation to the monoclinic HfO_2 phase had initiated after heat treatment at about 1200^0C for

moderate period. It has been confirmed by EXAFS studies that part of the film maintained still amorphous phase when heat treated at 1100^0C for a long period.

Composite thin films consisting of high-index and low-index materials have also major role in the optical coating technology because of their of refractive index tunability property[47]. Using composite thin films it has been possible to design thin film devices with minimum number of layers in the stack. Studies on the optical properties of (HfO_2:MgF_2) composite thin films deposited by electron beam evaporation [46] have shown the refractive index variation in the range 1.38 to 1.91 for various deposition ratios corresponding to 550 nm wavelength. Extensive studies have been made on morphology, grain structure and optical properties of co-evaporated thin films of (HfO_2:SiO_2) deposited by reactive electron beam evaporation on quartz substrate [48]. In course of these studies, films have been grown with by varying (HfO_2:SiO_2) composition and phase modulated ellipsometry and AFM have been successfully used to determine their refractive index and surface roughness variations respectively. It has been reported that the films with lower silica percentage composition have improved refractive indices and band gaps, superior surface roughness as well as denser morphology as compared to those of the pure hafnia film. In this report, we have discussed the microstructure and the local structure of pure hafnium oxide thin film and composite thin films having varying hafnia and silica compositions as prepared by reactive electron beam evaporation. XRD and EXAFS measurements on these films have been carried out for estimating the microstructure and the local structure around hafnium atom.

2. Experiment

Several thin films samples of hafnium oxide and composite (HfO_2:SiO_2) were deposited in a fully automatic box coating unit VERA-902 [48]. This coating system contains two 8kW electron beam guns and two resistance sources which have been interfaced with the process controller along with Inficon's XTC/2 quartz crystal monitors as well as Leybold's OMS optical thickness monitor. Using various in-built and user defined programs, the sources can be simultaneously operated to carry out the co-deposition process. A cold cathode ion gun, Denton's model CC102 is provided in the coating system for performing ion beam cleaning as well as ion assisted deposition (IAD). The rates of evaporation from individual sources is detected dynamically and controlled to an accuracy better than 0.1 nm/sec while using the crystal monitors. The deposition of the films was carried out using the electron gun with sweep and automatic emission control. The coating materials HfO_2 and SiO_2 were chosen from Cerac's batches with a typical purity level of 99.9%. During the deposition process of the composite thin films, the quartz substrate temperature was maintained at 350^0C and the pressure was kept at $1x10^{-4}$ mbar by using MKS mass flow controller. The optical thickness of the thin films were maintained at 6-8 quarter waves corresponding to 600 nm. During the deposition process the evaporation rate was continuously monitored and controlled as required in the co-deposition process. In order to remove unwanted fluctuation in the rate of evaporation, proportional, differential and integrated parameters of the thickness as process control systems were optimized. Based on the accurate process control, hafnia percentage in the composite films of (HfO_2:SiO_2) was varied in the range of 0-100%.

XRD measurements on the thin film sample containing pure hafnia and composite thin films samples having varying hafnia and silica percentages were carried out using a versatile x-ray diffractometer (VXRD) setup [49]. The main assembly of VXRD is a diffractometer (D8 Discover, Bruker AXS) with Cu (sealed tube) source. A Göbel mirror is used after the source in order to select and enhance CuKα radiation (λ = 1.54 Å). The diffractometer uses a two-circle goniometer [$\theta(\omega)$-2 θ] with quarter-circle Eulerian cradle as sample stage. The latter has two circular (χ and φ) and three translational (X, Y and Z) motions. Scattered beam was detected using NaI scintillation (point) detector. Powder diffraction data were initially recorded by scanning both the incident angle (α) and the exit angle (β) equally (such that $\alpha = \beta = \theta$). Data collected in this way is sensitive to whole sample. Since the thickness of the sample is very small it was necessary to make the diffraction data sensitive to the top of the deposited film and powder diffraction data were recorded by keeping the incident angle fixed at grazing angle and scanning the exit angle such that $\beta = \theta$. Fixing the incident angle at grazing angle reduced the penetration depth and increased the illuminated area of the sample. In course of recording the data, the value of θ of was optimized at 0.4 degree.

EXAFS experiments on the above mentioned thin film samples were carried out at the BL17C1 beamline on the Twaiwan Light Source (1.5 Gev, 300 mA) which is located at the National Synchrotron Radiation Research Center, Hsinchu, Taiwan. The heart of the beamline is a Si(111) double crystal monochromator (DCM). During EXAFS experiments, all measurements were performed at the L_3 absorption-edge of hafnium. Since x-ray photons are absorbed when transmitted through the quartz substrate of the

thin films, the data were recorded in the fluorescent mode. Gas ionization chamber type detectors were used to record the incident photons on the experimental samples as well as the fluorescent photons from the samples.

3. Result and discussion

Fig.1(a) shows the recorded XRD pattern of the thin film sample made of 100% pure HfO_2 whereas Figs.1(b) to 1(d) are the recorded XRD patterns corresponding to the composite thin film samples having (HfO_2:SiO_2) composition as (90%:10%), (85%:15%) and (80%:20%) respectively. It may be seen from Fig.1(a) that pure hafnium oxide film has crystalline microstructure with several peaks. While comparing these peaks with powdered reference of hafnium oxide, it has been confirmed that the microstructure of the deposited pure hafnium oxide film is not monoclinic. The exact nature of the microstructure has, however, been established from the analysis of the EXAFS data. It may be further seen from Figs.1(b) to 1(d) that the composite thin films of (HfO_2:SiO_2) are amorphous having a broad peak in the XRD pattern. This broad peak which lies in the range of $(25^0\text{-}37^0)$ for 2θ is ascribed to the quartz substrate and amorphous hafnia.

The experimental data recorded at the L_3 absorption-edge of hafnium during EXAFS experiment on thin film samples prepared with pure hafnia as well as varying (HfO_2:SiO_2) composition were processed by the well known software program *ATHENA* [50] available under *IFEFFIT* package which first calculated the energy-dependent absorption coefficient $\mu(E)$. After atomic absorption background subtraction, the program converted the energy dependent absorption coefficient as a function of photoelectron wave-number, k, defined by $\hbar^2k^2/2m = E - E_0$, where E is the incoming X-ray photon energy and E_0 is the absorption threshold energy and m is the electron mass. This

photoelectron wave-number based absorption function $\chi(k)$ is called as EXAFS function. Finally, the EXAFS function $\chi(k)$'s are Fourier transformed (FT) using a Gaussian window for *k*-range of [2.0-8Å^{-1}] with a k^2 weighting in order to account the large *k*-region fully. The FT operation is done in the *R*-space, where *R* is the radial distance between the absorbing atom and the neighboring atom. For the pure HfO_2 thin film, Fig. 2(a) represents the typical energy dependent absorption curve. Fig. 2(b) represents the corresponding absorption curve in the *k*-space. Fig. 2(c) shows the plot of $\chi(R)$ which is FT version of EXAFS function $\chi(k)$ in the *R*-space. Finally, figs.[3(a)-3(c)], [4(a)-4(c)], [5(a)-5(c)], [6(a)-6(c)] show the energy dependent absorption curves (a), absorption curves in the *k*-space (b) and the plots of FT spectra in *R*-space (c) corresponding to composite thin films having varying (HfO_2:SiO_2) compositions of (90%:10%), (80%:20%), (70%:30%) and (50%:50%) respectively. Fig.7 shows the combined plot of FT spectra corresponding to pure HfO_2 and composite thin films with varying (HfO_2:SiO_2) compositions. It may be seen from this figure that the intensities as well as the widths of the first shell (Hf-O) and second shell (Hf-Hf) peaks increase with the variation of hafnia and silica concentrations when the thin film samples changes from amorphous to crystalline phase (see figs.1). The lowest value of the first shell peak intensity may, however, be noted with the film having small silica concentration of 10%. It may be, also, seen from fig.7 that the widths of the first shell and the second shell peaks are minimum for the film with this small silica concentration. When comparing the second shell peaks, it may be clearly observed that the peak intensity is lowest corresponding to the film with equal hafnia and silica concentrations. During EXAFS studies, similar results for the peak intensities and peak widths in the FT spectra of pulsed

laser deposited composite films of (HfO_2:ZrO_2) with the variation of hafnia and zirconia concentrations have also been reported [16]. As reported in reference [48], two dimensional AFM images of (HfO_2:SiO_2) composite thin films have depicted small grain structure for the film with lower silica concentration. Therefore, the above mentioned small peak widths in the FT spectrum corresponding to lower silica concentration in the (HfO_2:SiO_2) composite thin film is attributed to the small grain structure in the film.

Detailed analysis of FT spectra in the *R*-space has been carried out in order to extract the information on the distance of the neighbouring atom (*R*), coordination number of the neighbouring atom (*N*) and mean-square disorder of neighbour distance (σ^2) around the hafnium atom. While analyzing the FT spectra, the software program *ARTEMIS* [50] available under *IFEFFIT* package have been extensively used to fit the Fourier transformed EXAFS spectra with the theoretical spectra which are calculated based on the possible crystal phases of HfO_2 and its lattice parameters and fractional coordinates obtained from the literature. It has been reported in [5,45] that thin films of pure HfO_2 show various crystalline phases, namely, monoclinic, orthorhombic, tetragonal, cubic phases, etc. during post deposition annealing. Polycrystalline phases of pure HfO_2 have, also, been identified when films are grown by chemical vapour deposition [8] and atomic layer deposited films are subjected to rapid thermal annealing [3]. Initially, we have considered all the single crystalline phases separately for carrying out the fitting work. Figs.8, 9 and 10 show the fittings of the FT spectra with the theoretically calculated spectra corresponding to pure HfO_2 thin film when monoclinic, orthorhombic and tetragonal phases are considered respectively. It may be clearly seen that none of the pure crystalline models has been able to give good fitting result.

Subsequently, we have considered the polycrystalline model of pure HfO_2 thin film consisting of monoclinic, orthorhombic and tetragonal phases. Fig.11 shows the fitting result when combined monoclinic and orthorhombic phases are considered. It may be seen from this figure that the fitting of the FT spectrum with the theoretical spectrum is yet to be improved. Finally, the best fitting result shown in Fig.12 has been achieved when mixed composition of monoclinic, orthorhombic and tetragonal phases is considered. It may be seen from this figure that the fitted FT spectrum is multiply structured with three broad peaks. As extracted from the fitting results, the peak with highest intensity corresponds to the Hf-O bond whereas the remaining two peaks correspond to two separate Hf-Hf bonds. Thus the long range ordering shown by the multiple structure in the fitted FT spectrum has further established the crystalline microstructure of the pure HfO_2 thin film with mixed composition of monoclinic, orthorhombic and tetragonal phases.

Figs.13 to 16 show the fitting of the FT spectra with the theoretically calculated spectra corresponding to composite thin films having varying (HfO_2:SiO_2) compositions of (90%:10%), (80%:20%), (70%:30%) and (50%:50%) respectively. It may be seen from these figures that the fitted FT spectra have only two broad peaks. As discussed earlier, the peaks with higher and lower intensities corresponds to Hf-O and Hf-Hf bonds respectively. The limited number of broad peaks in the FT spectra is correlated with the short range ordering which confirms the amorphous structure of these composite thin films. It has been discussed in reference [6] that when the measured first-shell (Hf-O) intensities in the FT spectra of amorphous (*a*-HfO_2) and crystalline (*c*-HfO_2) are almost identical, the number of near neighbours and the disorder along the Hf-O bond direction

in *a*-HfO_2 are similar to those in *c*-HfO_2. Therefore, the local structure of the *a*-HfO_2 film has been analyzed on the basis of monoclinic local structure of *c*-HfO_2. It may be seen from Fig.7 that the measured first-shell intensities in the FT spectra of the current *c*-HfO_2 and amorphous (HfO_2:SiO_2) thin films are more or less similar. We have, therefore, analyzed the local structure of amorphous (HfO_2:SiO_2) thin films around Hf atom on the basis of the mixed crystalline local structure of pure HfO_2 thin film. As discussed earlier, the mixed crystalline local structure consists of monoclinic, orthorhombic and tetragonal phases.

The results obtained through the EXAFS analysis of the FT spectra corresponding to pure HfO_2 thin film having polycrystalline microstructure and amorphous (HfO_2:SiO_2) thin films as discussed above, have been summarized in Table.1. EXAFS studies on pure HfO_2 thin films [5,6,14,16,17] , HfSiO thin film[11] and composite (HfO_2:SiO_2) thin film [45] prepared by various deposition methods and subjected to post deposition annealing have shown variations of the bond length (*R*) and coordination number (*N*) corresponding to (Hf-O) and (Hf-Hf) shells. The same has been observed when the results shown in Table.1 have been compared with the published data corresponding to the atomic layer deposited thin films [6] and the film deposited by sol-gel method [45]. The (Hf-O) and (Hf-Hf) bond lengths corresponding to the amorphous thin films having (HfO_2:SiO_2) compositions of (90%:10%) and (70%:30%) shown in Table.1 are more or less similar to those for the amorphous and partially amorphous thin films as reported in [6] and [45] respectively. Also, the first shell (Hf-O) coordination numbers (7 and 6) corresponding to amorphous thin films having (HfO_2:SiO_2) compositions of (90%:10%) and (70%:30%) respectively, are identical to those for the above mentioned amorphous and partially

amorphous thin films. However, the second shell (Hf-Hf) coordination numbers (7 and 6) shown in Table.1 are not identical to the reported values corresponding to the amorphous and partially amorphous thin films referred above. Although the first shell (Hf-O) and the second shell (Hf-Hf) coordination numbers (7 and 7) shown in Table.1 corresponding to pure HfO_2 thin film having polycrystalline microstructure are identical to those for the polycrystalline HfO_2 reported in [45], the (Hf-O) and (Hf-Hf) bond lengths are slightly different for the two cases.

It may be seen from Table.1 that as the silica percentage in the $(HfO:SiO_2)$ thin film varies in the range 0-50% , both the (Hf-O) and (Hf-Hf) bond lengths vary. The minimum values for these bond lengths correspond to the film having $(HfO:SiO_2)$ composition of (90%:10%). The variation of the measured refractive index with the variation of $(HfO:SiO_2)$ composition in the thin film and the highest value of the refractive index corresponding to the film having $(HfO:SiO_2)$ composition of (90%:10%) has been reported in [48]. Considering amorphous $(HfO:SiO_2)$ thin film having finite silica percentage composition, it may be seen from Table.1 that the bond lengths increase as silica percentage increases from 10% to 50%. As reported in [48], the refractive index of the amorphous $(HfO:SiO_2)$ thin film decreases along with the increase of band gap when the silica percentage increases from 10% to 50%. Although, the respective (Hf-O) and (Hf-Hf) bond lengths corresponding to the first and the second coordination shells are more or less identical in the cases of pure HfO_2 film and composite film having $(HfO:SiO_2)$ composition of (50%-50%), the refractive indices of these two films are not equal. This may be due to the fact that the additional (Hf-Hf) bonding corresponding to

the third coordination shell present in the case of pure HfO_2 film is missing in the case of composite thin film.

Therefore, we have arrived at the following conclusions for amorphous (HfO_2:SiO_2) thin film when the results of the present EXAFS study is correlated with those of the ellipsometric studies reported in [48].

(1) Refractive index is maximum and (Hf-O) and (Hf-Hf) bond lengths are minimum when silica percentage is 10%.

(2) As the silica percentage increases from 10% to 50%,

(a) (Hf-O) and (Hf-Hf) bond lengths increase.

(b) Refractive index decrease.

(c) Dielectric constant decrease.

(d) Band gap increase.

It has been reported that for most investigated high *K* materials [51,53], the band gap is roughly inversely proportional to the dielectric constant. As the dielectric constant increases, the band gap decreases. Decreasing of refractive index and dielectric constant along with increasing (Si-Si) bond length has been reported in the case of ion plated SiO_2 film [52], when the film is successively annealed in N_2 ambient with increasing anneal temperature. Decreasing of refractive index with increasing silica percentage have also been observed in (TiO_2:SiO_2) composite thin films [47] prepared by co-deposition technique. Finally, EXAFS studies on the Ti-Si binary oxide thin films [54] prepared by using an ionized cluster beam deposition method have shown the change in local structure with the change in TiO_2 content. It has been reported that (Ti-O) bond length increases with increasing TiO_2 percentage in the Ti-Si binary oxide thin films in which

the TiO_2 species are highly dispersed within the SiO_2 matrixes. In the case of (HfO_2:SiO_2) composite thin films SiO_2 species are most probably dispersed in HfO_2 matrixes. This is may be the reason for the similarity of the bond length changes in the (HfO_2:SiO_2) composite thin films and Ti-Si binary oxide thin films with changes of SiO_2 and TiO_2 concentrations respectively.

Acknowledgement

One of the authors, N. C. Das, sincerely acknowledges the generous financial support from DAE-BRNS under Raja Ramanna Fellowship Scheme during the course of the work. We acknowledge Dr. S. Banerjee and Dr. M. K. Sanyal, Director, SINP for their cooperation throughout the course of the work. We also thank Dr. B. K. Ankush for helping in the graphics work.

References

1. G. D. Wilk, R. M. Wallace and J. M. Anthony, J. Appl. Phys. **89**, 5243 (2001).

2. J. Robertson, Rep. Prog. Phys. **69**, 327 (2006).

3. P. S. Lysaght, P. J. Chen, R. Bergmann, T. Messina, R. W. Murto, H. R. Huff, J. Non-Crystalline Solids. **303**,54 (2002).

4. J.-F. Damlencourt, O. Renault, D. Samour, A.-M. Papon, C. Leroux, F. Martin, S. Marthon, M.-N. Semeria, X. Garros, Solid-State Electronics, **47**, 1613(2003).

5. Patric S. Lysaght, Joseph C. Woicik, M. Alper Sahiner, Byoung-Hun Lee, Raj Jammy, Appl. Phys. Lett. **91**, 122910 (2007).

6. Deok-Yong Cho, Tae Joo Park, Kwang Duk Na, Jeong Hwan Kim, and Cheol Seong Hwang, Phy. Rev. B **78,** 132102 (2008).

7. Q. Fang, J.-Y. Zhang, Z. M. Wang, J. X. Wu, B. J. O'Sullivan, P. K. Hurley, T. L. Leedham, H. Davis, M. A. Audier, C. Jimenez, J.-P. Senateur, Ian W. Boyd, Thin Solid Films. **427**, 391 (2003).

8. R. C. Smith, T. Ma, N. Hoilien, L. Y. Tsung, M. J. Bevan, L. Colombo, J. Roberts, S. A. Campbell, W. L. Gladfelter, Adv. Mater. Opt. Electron. **10**, 105 (2000).

9. Q. Fang, J. Y. Zang, Z. M. Wang, G. He, J. Yu, Ian W. Boyd, Microelectronic Engineering, **66**, 621 (2003).

10. T. Nishide, S. Honda, M. Matsuura, M. Ide, Thin Solid Films, **371**, 61 (2000).

11. J. Moris, L.Miotti, K. P. Bastos, S. R. Teixeira, I. J. R. Baumvol, A. L. P. Rotondaro, J. J. Chambers, M. R. Visokay, L. Colombo, M. C. Martins Alves, Appl. Phys. Lett. **86**, 212906 (2005).

12. P.F. Lee, J.Y. Dai, H.L.W. Chan, C.L. Choy, Ceramics International, **30**, 1264(2004).

13. M. Ratzke, D. wolfframm, M. Kappa, S. Kouteva-Arguirova, J. Reif, Appl. Surf. Sci. **247**, 128 (2005).

14. Deok-Yong Cho, C.-H. Min, Jungho Kim, S.-J. Oh, Appl. Phys. Lett. **89,** 253510, (2006).

15. M. Filipescu, N. Scarisoreanu, V. Cracium, B. Mitu, A. Purice, A. Moldovan, V. Ion, O. Toma, M. Dinescu, Appl. Surf. Sc. **253**, 8184(2007).

16. Mehmet Alper Sahiner, Joseph C. Woicik, Peng Gao, Patric McKeown, Mark C. Croft, Michael Gartman, Brendan Benapfla, Thin Solid Films, **515**, 6548 (2007).

17. Mehmet Alper Sahiner, Joseph C. Woicik, Timothy Kurp. Jeffrey Serfass, Marc Aranguren, Mat. Sci. Semicond. Process. (2008), doi:10.1016/j.mssp.2008.08.003

18. Vladimir Gritsenko, Daryja Gritsenko, Sergei Shaimeev, Vladimir Aliev, Kamil Nasyrov, Simon Erenburg, Vladimir Tapilin, Hei Wong, M.C. Poon, J.H.Lee, J.-W. Lee, C.W. Kim, Microelectronic Engineering, **81,** 524 (2005).

19. M. Zukic, D. G. Torr, J. F. Spann, M. R. Torr, Appl. Opt. **28**, 4284 (1990).

20. F. Y. Genin, C. J. Stolz, Proc. SPIE, **2870**, 439 (1996).

21. M. Fadel, O. A. Azim M., O. A. Omer, R. R. Basily, Appl. Phys. **A66**, 3 (1998).

22. Yongjin Wang, Zhilang Lin, Xinli Cheng, Haibo Xiao, Feng Zhang, Shichang Zou, Appl. Surf. Sci. **228**, 93 (2004).

23. M. F. Al-Kuhaili, Opt. Mat. **27**, 383 (2004).

24. M. Jerman, Z. Qiao, D. Mergel, Appl. Opt. **44**, 3006 (2005).

25. M. Alvisi. M. Di Giulio, S. G. Marrone, M. R. Perrone, M. L. Protopapa, A. Valentini, L. Vasanelli, Thin Solid Films, **358**, 250 (2000).

26. T. R. Jensen, R. L. Johnson,Jr., J. Ballou, W. Prohaska, S. E. Morin, Soc.Vacu. Coaters 43rd Annual Tech. Conf. Proc.**505**, 239-243 (2000)

27. B. Andre, L. Poupinet, G. Ravel, J. Vac. Sci.Technol. A **18(5)**, 2372 (2000).

28. M. Alvisi, F. De Tomasi, M. R. Perrone, M. L. Protopapa, A. Rizzo, F. Sarto, S. Scaglione, Thin Solid Films, **396**, 44 (2001).

29. D. E. Morton, T. R. Jensen
http://www.dentonvacuum.com/PDFs/Tech_papers/moisture.PDF

30. T. R. Jensen, J. Warren, R. L. Johnson,Jr. Appl. Opt. **41**,3025 (2002).

31. J. Wang, R. L. Maier, H. Schreiber, Appl. Opt. **47**, C189 (2008).

32. R. Chow, S. Falabella, G. E. Loomis, F. Rainer, C. J. Stolz, M. R. Kozlowski, Appl. Opt. **32**, 5567 (1993).

33. S. C. Weakly, C. J. Stolz, Z. Wu, R. P. Bevis, M. K. Von Gunten, Proc. SPIE, **3578**, 137 (1999).

34. S. M. Edlou, A. Smajkiewicz, G. A. Al-Jumaily, Appl. Opt. **32**, 5601 (1993).

35. P. Torchio, A. Gatto, M. Alvisi, G. Albrand, N. Kaiser, C. Amra, Appl. Opt. **41**,3256 (2002).

36. J. M. Khoshman, M. E. Kordesch, Surf. Coat. Technol. **201**, 3530 (2006).

37. L. Gallais, J. Capoulade, J. Y. Natoli, M. Commandre, M. Cathelinaud, C. Koc, M. Leguime, Appl. Opt. **47**, C107 (2008).

38. J. M. Khoshman, A. Khan, M. E. Kordesch, Surf. Coat. Technol. **202**, 2500 (2008).

39. M. L. Grilli, F. Menchini, A. Piegari, D. Alderighi, G. Toci, M. Vannini, Thin Solid Films, **517**, 1731 (2009).

40. D. J. Kranjnovich, M. Kulkarni, W. Leung, A. C. Tam, A. Spool, B. York, Appl. Opt. **31**,6062 (1992).

41. C. Giuri, M. R. Perrone, V.Piccinno, Appl. Opt. **36**, 1143 (1997).

42. G. D. Wilk, R. M. Wallace and J. M. Anthony, J. Appl. Phys. **87**, 484 (2000).

43. D. A. Neumayer and E. Cartier, J. Appl. Phys. **90**, 1801 (2001).

44. L. Armelao, D. Bleiner, V. Di Noto, S. Gross, C. Sada, U. Schubert, E. Tondello, H. Vonmont, A. Zattin, Appl. Surf. Sci. **249**, 277 (2005).

45. N. D. Afify, G. Dalba, U. M. K. Koppolu, C. Armellini, Y. Jestin, F. Rocca, Mat. Sc. Semicond. Proces. **9**, 1043 (2006).

46. Y. Tsou, F. C. Ho, Appl. Opt. **35**, 5091 (1996).

47. N. K. Sahoo, S. Thakur, D. Bhattacharyya, N. C. Das, Report BARC/1999/E/039, (1999), pp. 1-33.

48. R. B. Tokas, N. K. Sahoo, S. Thakur, N. M. Kamble, Curr. Appl. Phys. **8**, 589 (2008).

49. S. Hazra, Appl. Surf. Sc. **253**, 2154 (2006).

50. B. Ravel and M. Newville, J. Synchrotron Rad. **12**, 537 (2005).

51. J. Robertson, J. Vac. Sci. Technol. **B 18(3)**, 1785 (2000).

52. C.-F. Yeh, T.-J. Chen, Appl. Phys. Lett. **70(12)**, 1611 (1997).

53. H. Wong, B. Sen. V. Filip, M. C. Poon, Thin Solid Films. 504, 192 (2006).

54. M. Takeuchi, S. Dohshi, T. Eura, M. Anpo, J. Phys. Chem. B, **107**, 14278 (2003).

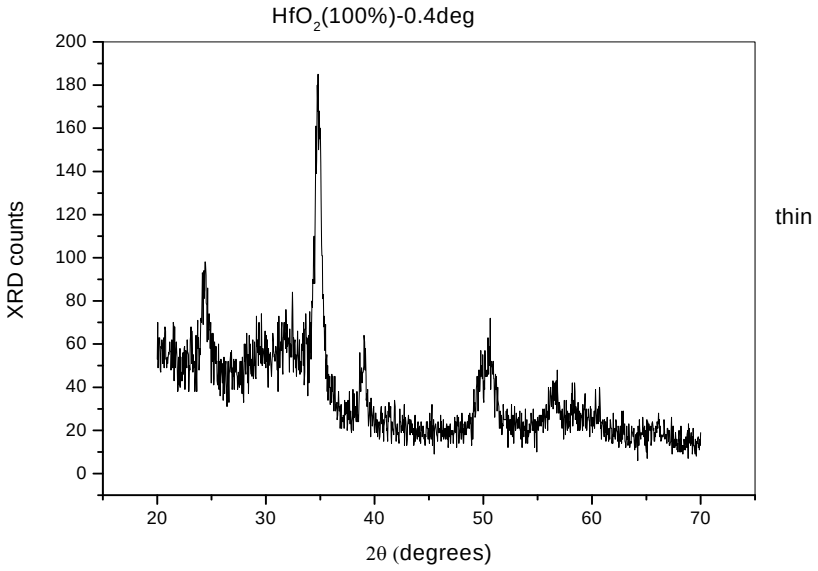

Fig.1(a): XRD pattern of pure HfO_2 thin film

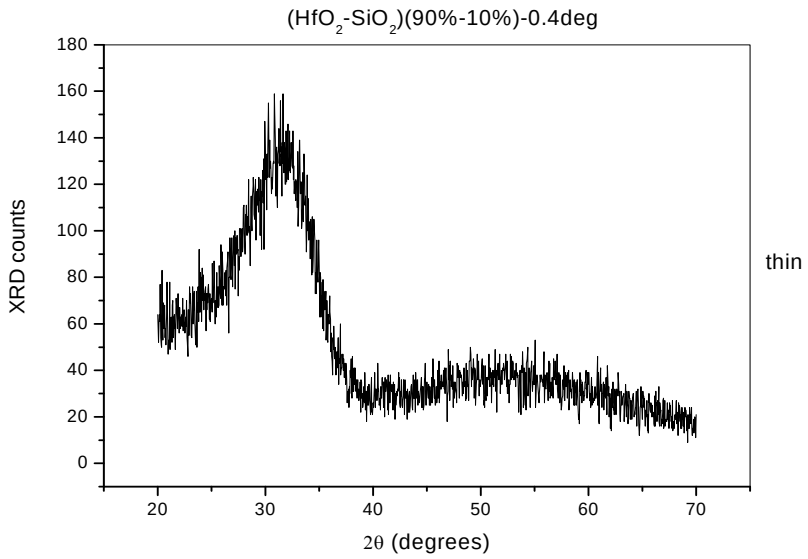

Fig.1(b): XRD pattern of composite thin film with (HfO_2:SiO_2) composition of (90%:10%)

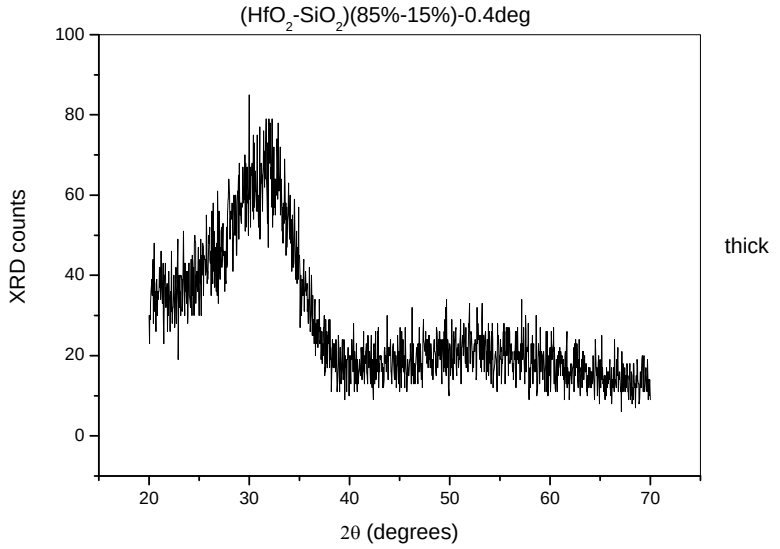

Fig.1(c): XRD pattern of composite thin film with (HfO_2:SiO_2) composition of (85%:15%)

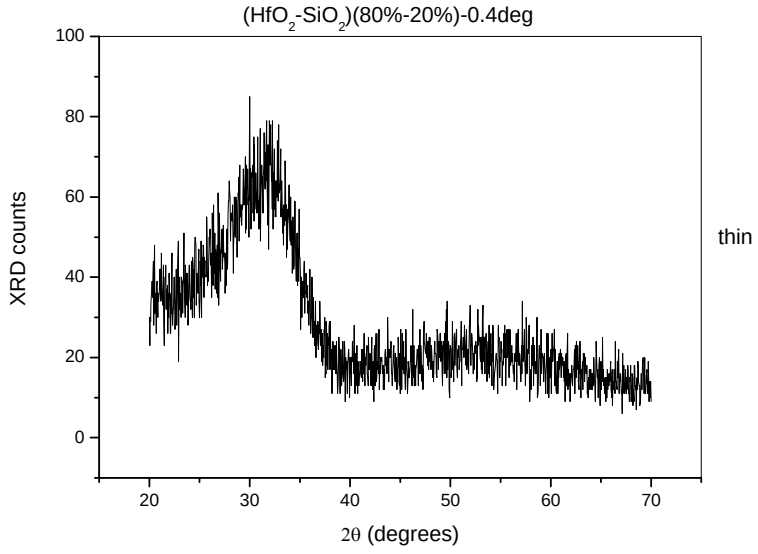

Fig.1(d): XRD pattern of composite thin film with (HfO_2:SiO_2) composition of (80%:20%)

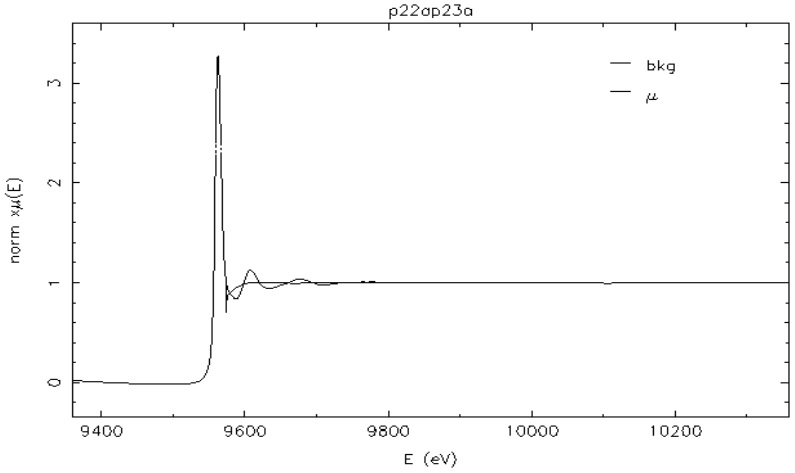

Fig.2(a): Energy dependent absorption curve of 100% HfO_2 film

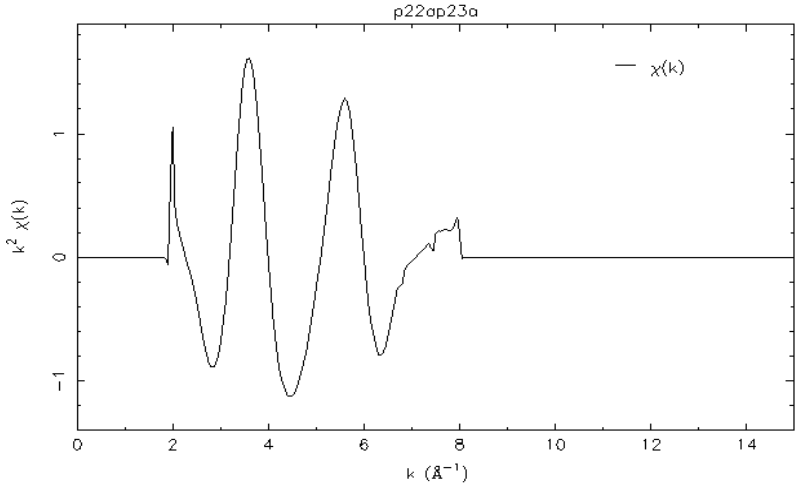

Fig.2(b): Weighted absorption curve in k-space for 100% HfO_2 film

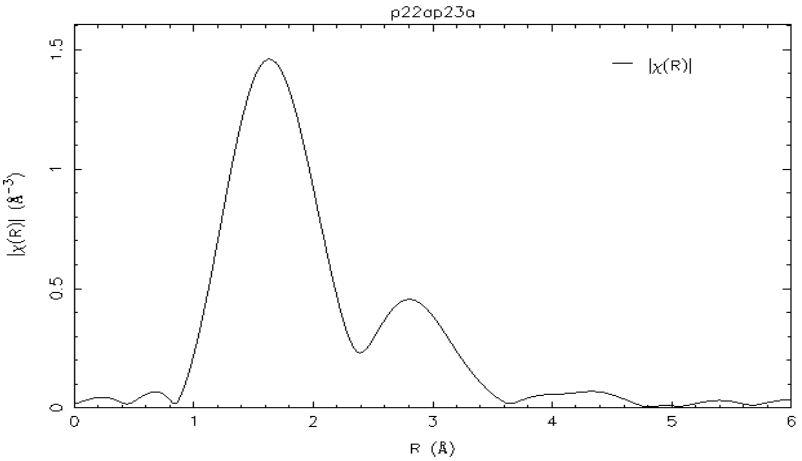

Fig.2(c): Plot of Fourier transformed [$k^2\chi(k)$] in R-space for 100% HfO_2 film

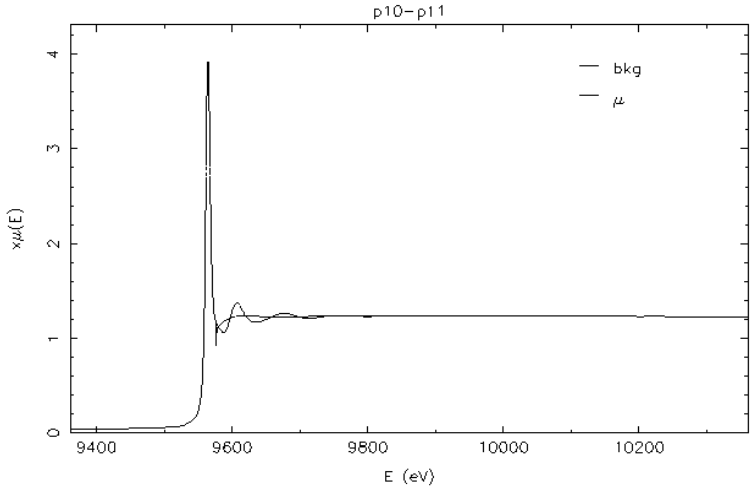

Fig.3(a): Energy dependent absorption curve for (90%:10%)(HfO_2:SiO_2) film

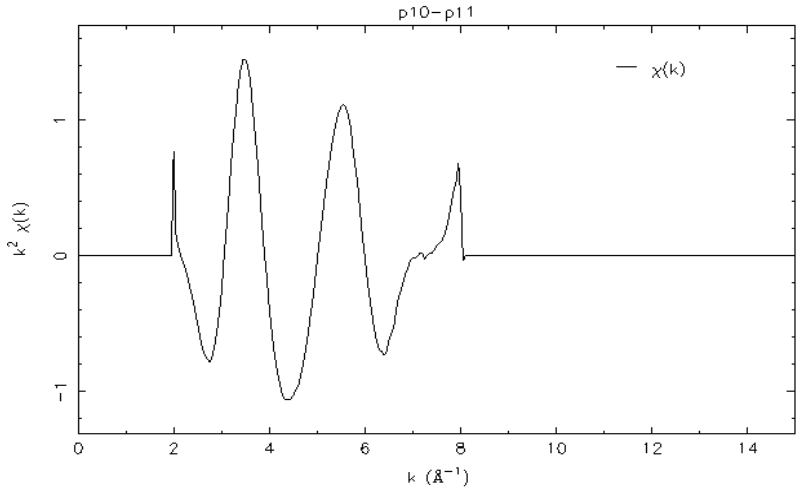

Fig.3(b): Weighted absorption curve in k-space for (90%:10%)(HfO_2:SiO_2) film

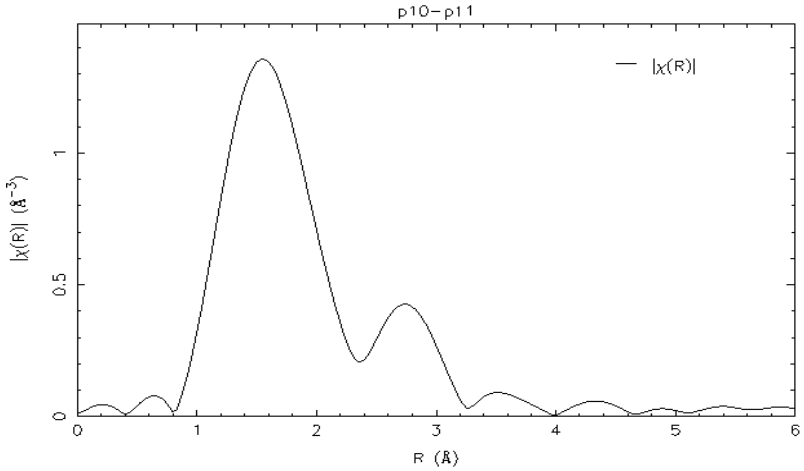

Fig.3(c): Plot of Fourier transformed [$k^2\chi(k)$] in R-space for (90%:10%)(HfO_2:SiO_2) film

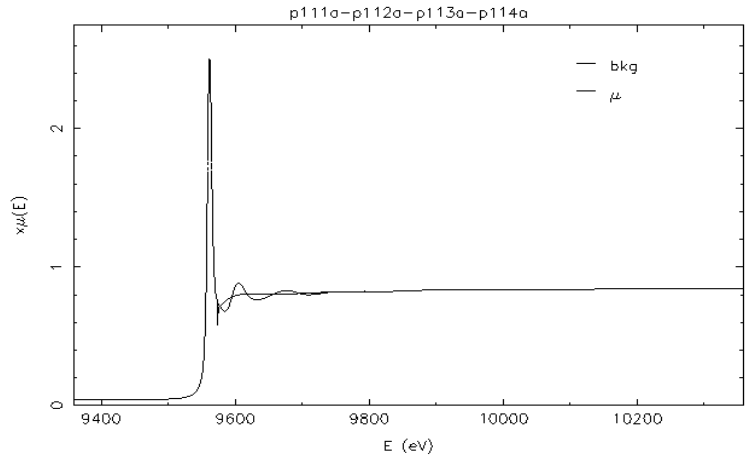

Fig.4(a): Energy dependent absorption curve for (80%:20%)(HfO_2:SiO_2) film

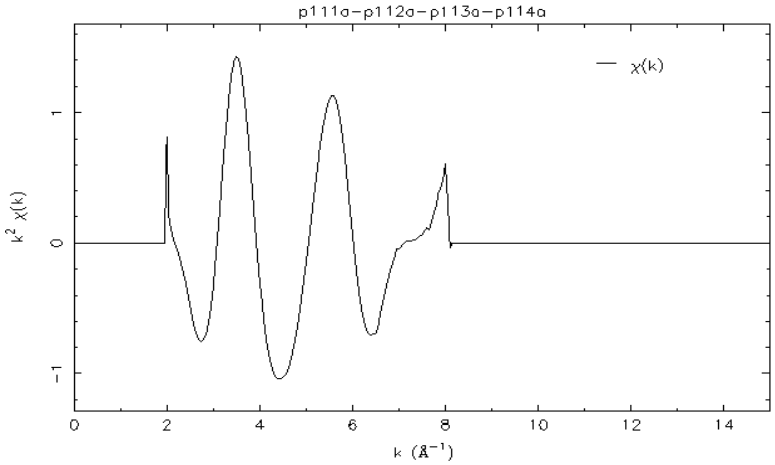

Fig.4(b): Weighted absorption curve in k-space for (80%:20%)(HfO_2:SiO_2) film

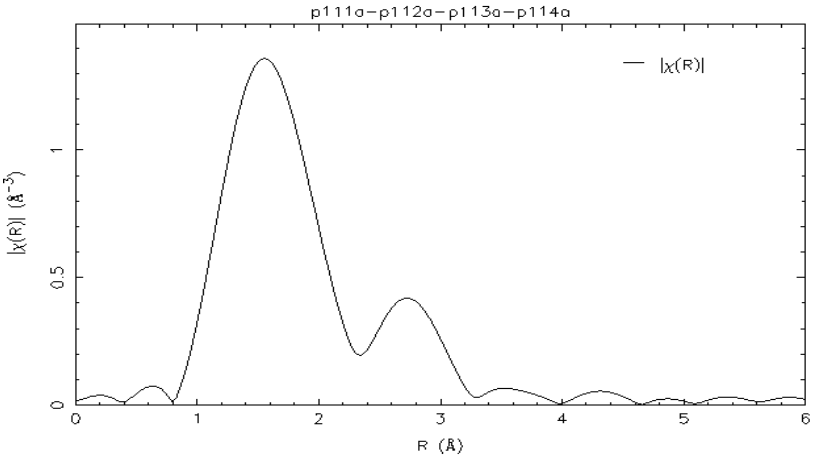

Fig.4(c): Plot of Fourier transformed [$k^2\chi(k)$] in R-space for (80%:20%)(HfO_2:SiO_2) film

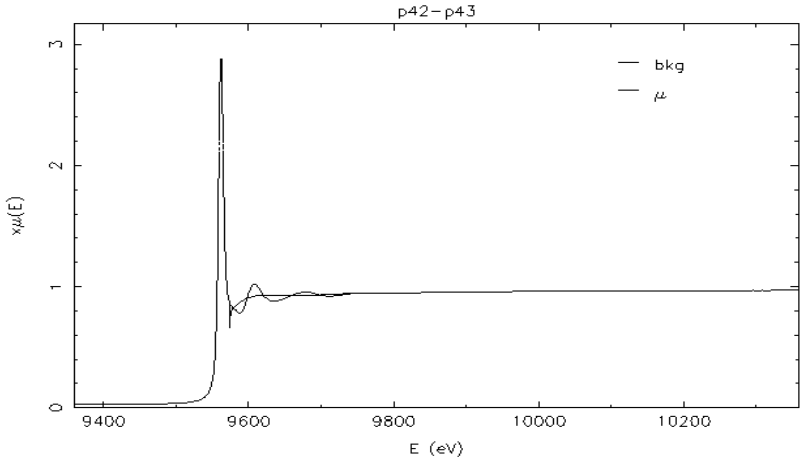

Fig.5(a): Energy dependent absorption curve for (70%:30%)(HfO_2:SiO_2) film

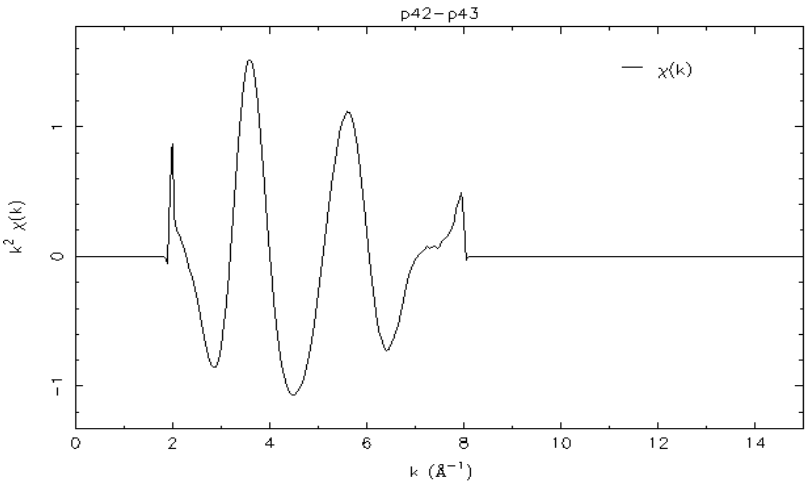

Fig.5(b): Weighted absorption curve in k-space for (70%:30%)(HfO_2:SiO_2) film

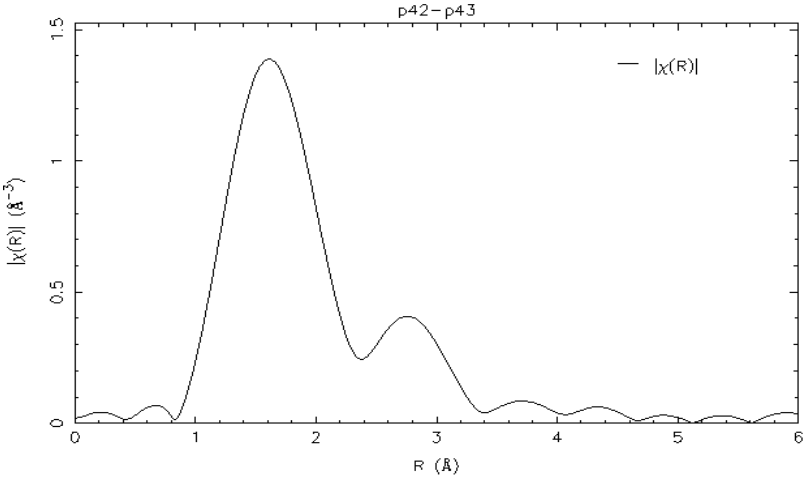

Fig.5(c): Plot of Fourier transformed [$k^2\chi(k)$] in R-space for (70%:30%)(HfO_2:SiO_2) film

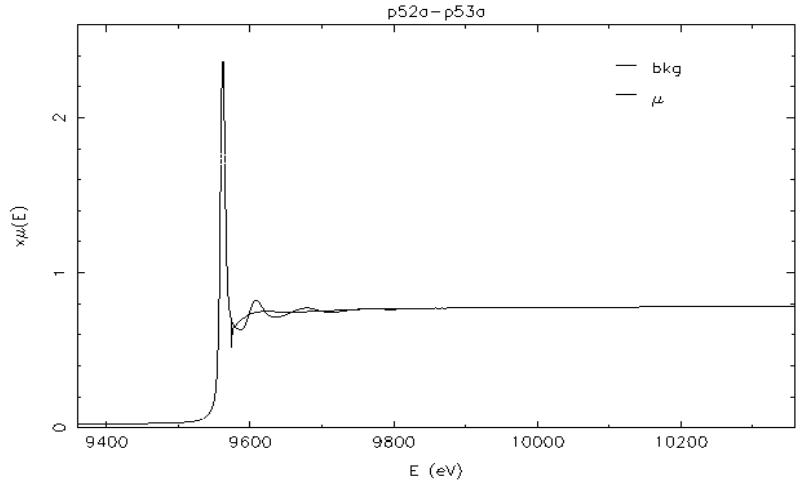

Fig.6(a): Energy dependent absorption curve for (50%:50%)(HfO_2:SiO_2) film

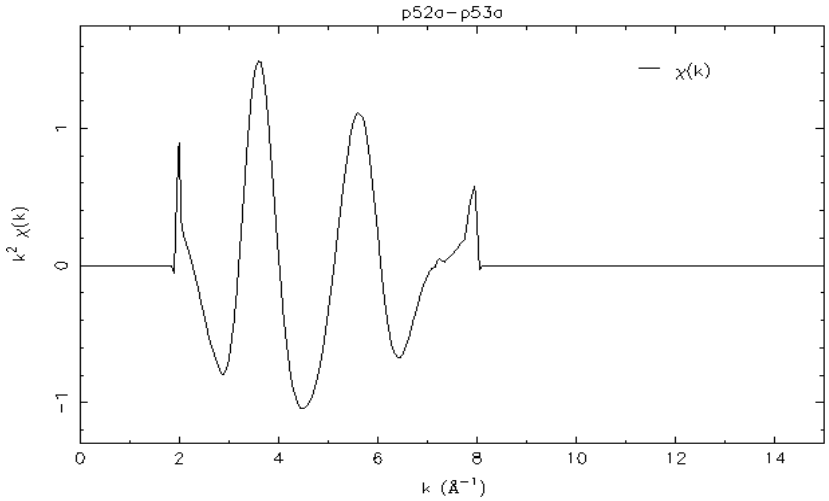

Fig.6(b): Weighted absorption curve in k-space for (50%:50%)(HfO_2:SiO_2) film

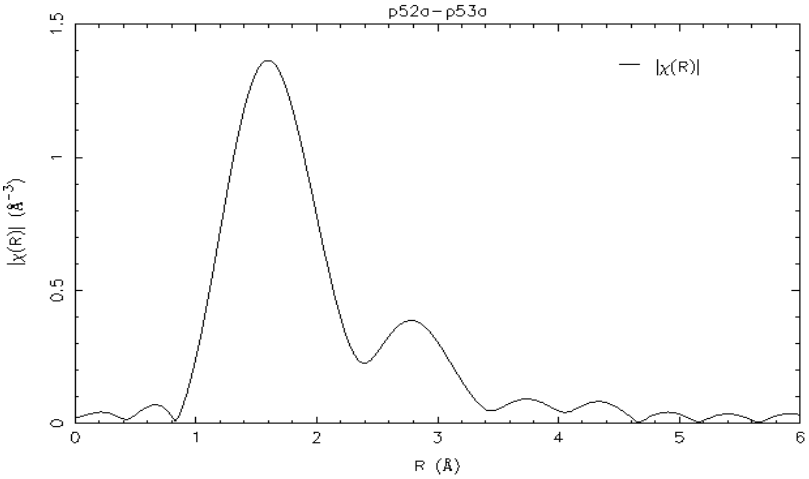

Fig.6(c): Plot of Fourier transformed [$k^2\chi(k)$] in R-space for (50%:50%)(HfO_2:SiO_2) film

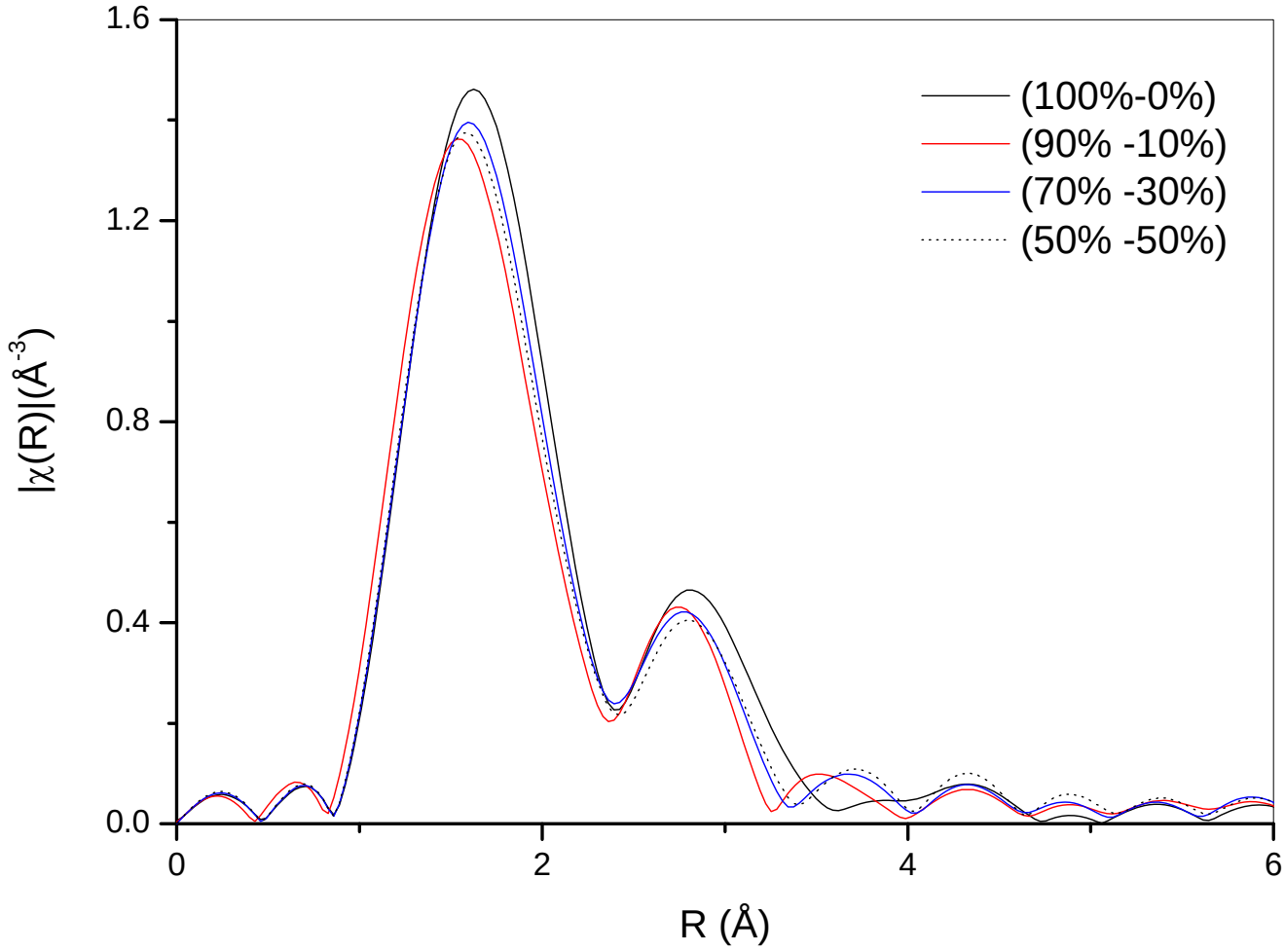

Fig.7: Combined plots of FT spectra in *R*-space corresponding to pure HfO_2 and Composite thin films with varying (HfO_2:SiO_2) compositions of (90%:10%), (70%:30%) and (50%:50%)

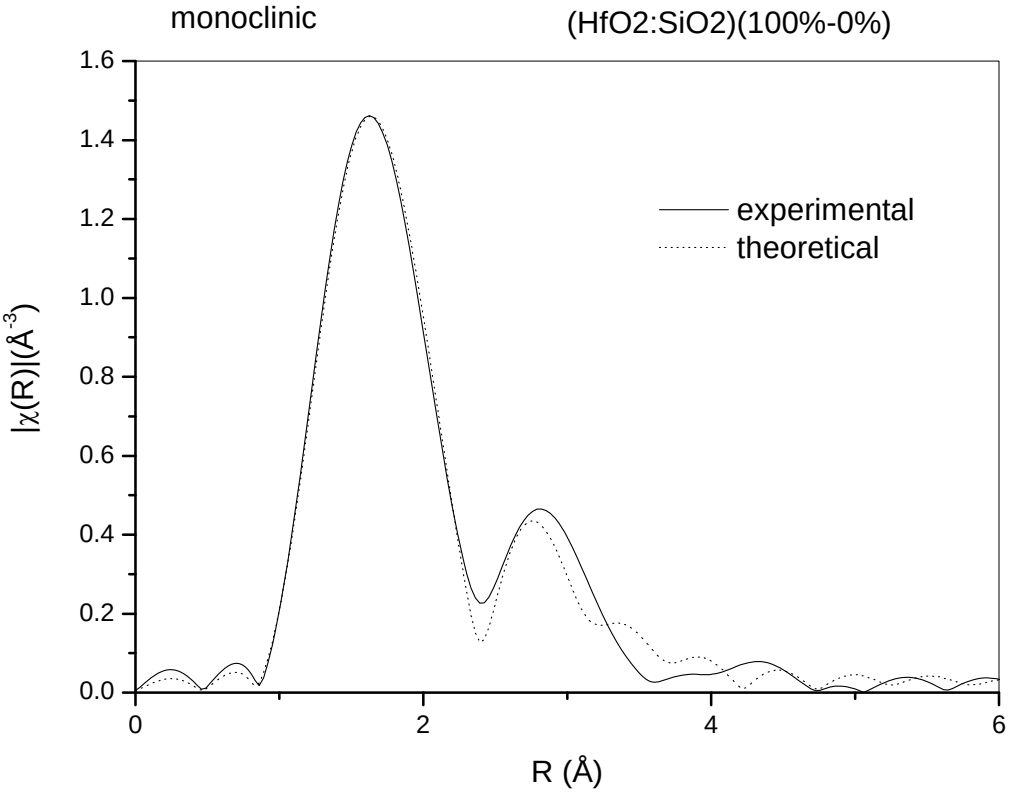

Fig.8: Fitting of FT spectrum in *R*-space with the theoretical spectrum corresponding to pure HfO_2 thin film based on pure monoclinic phase

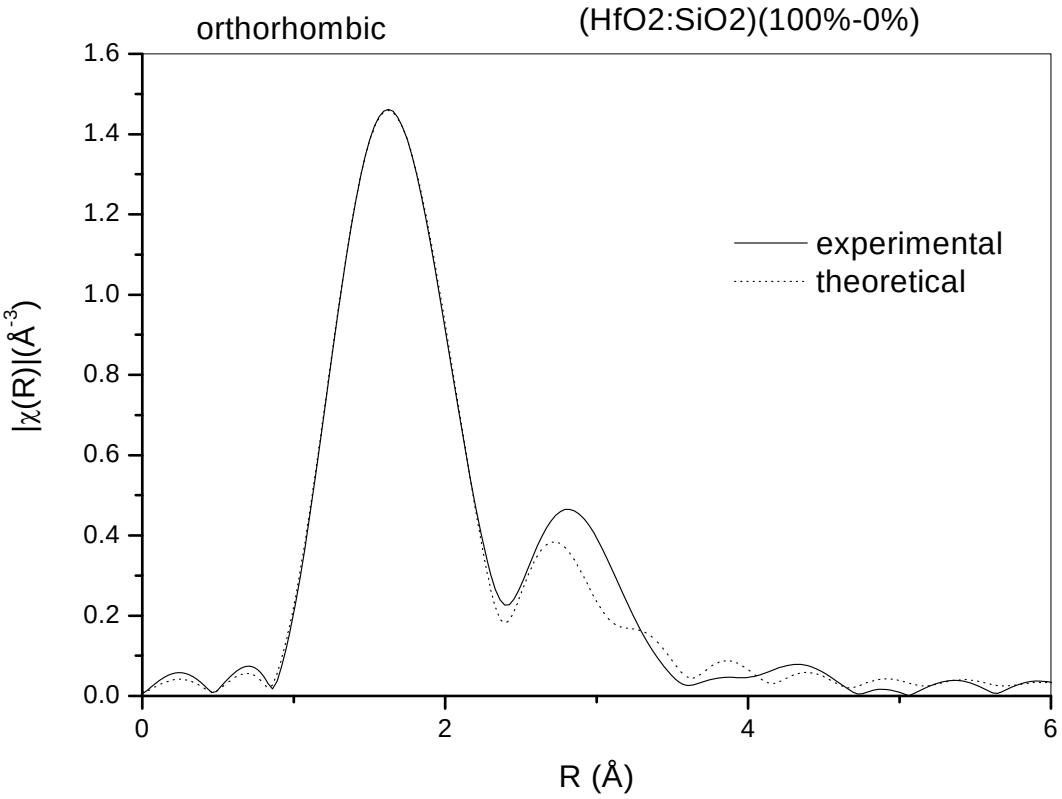

Fig.9: Fitting of FT spectrum in *R*-space with the theoretical spectrum corresponding to pure HfO_2 thin film based on pure orthorhombic phase

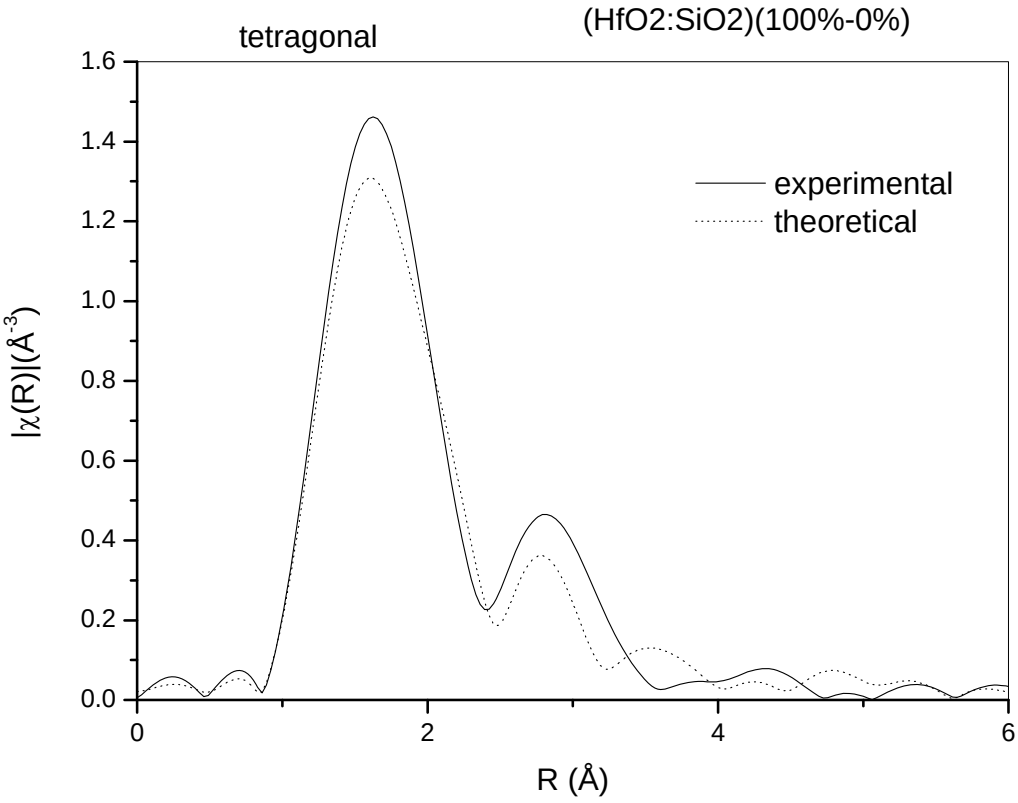

Fig.10: Fitting of FT spectrum in *R*-space with the theoretical spectrum corresponding to pure HfO_2 thin film based on pure tetragonal phase

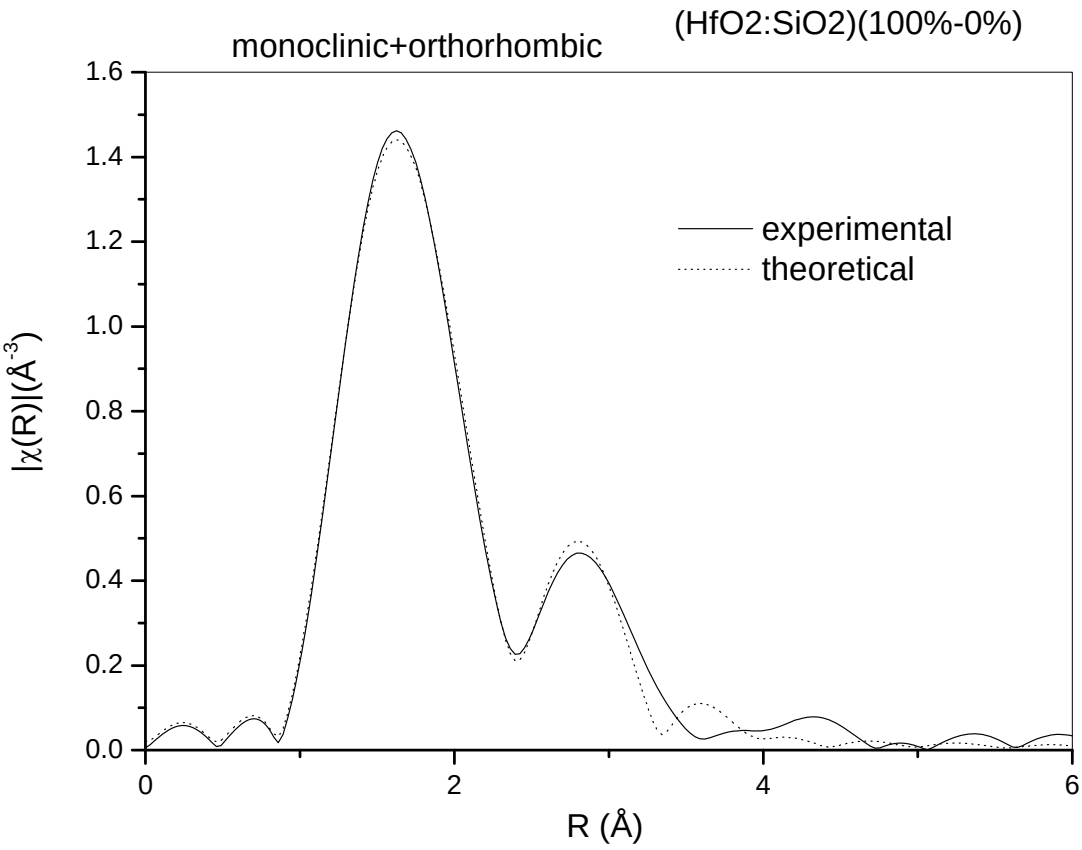

Fig.11: Fitting of FT spectrum in *R*-space with the theoretical spectrum corresponding to pure HfO_2 thin film based on combined monoclinic and orthorhombic phases

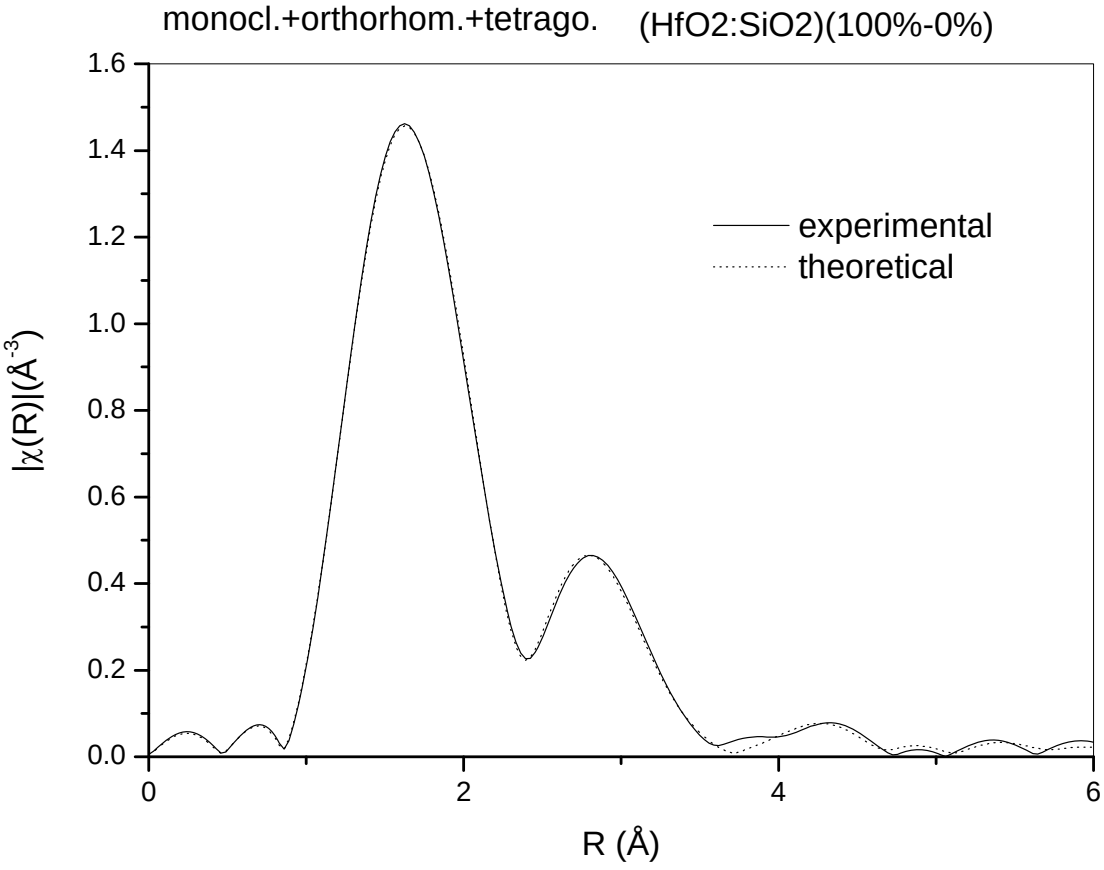

Fig.12: Fitting of FT spectrum in *R*-space with the theoretical spectrum corresponding to pure HfO_2 thin film based on combined monoclinic, orthorhombic and tetragonal phases

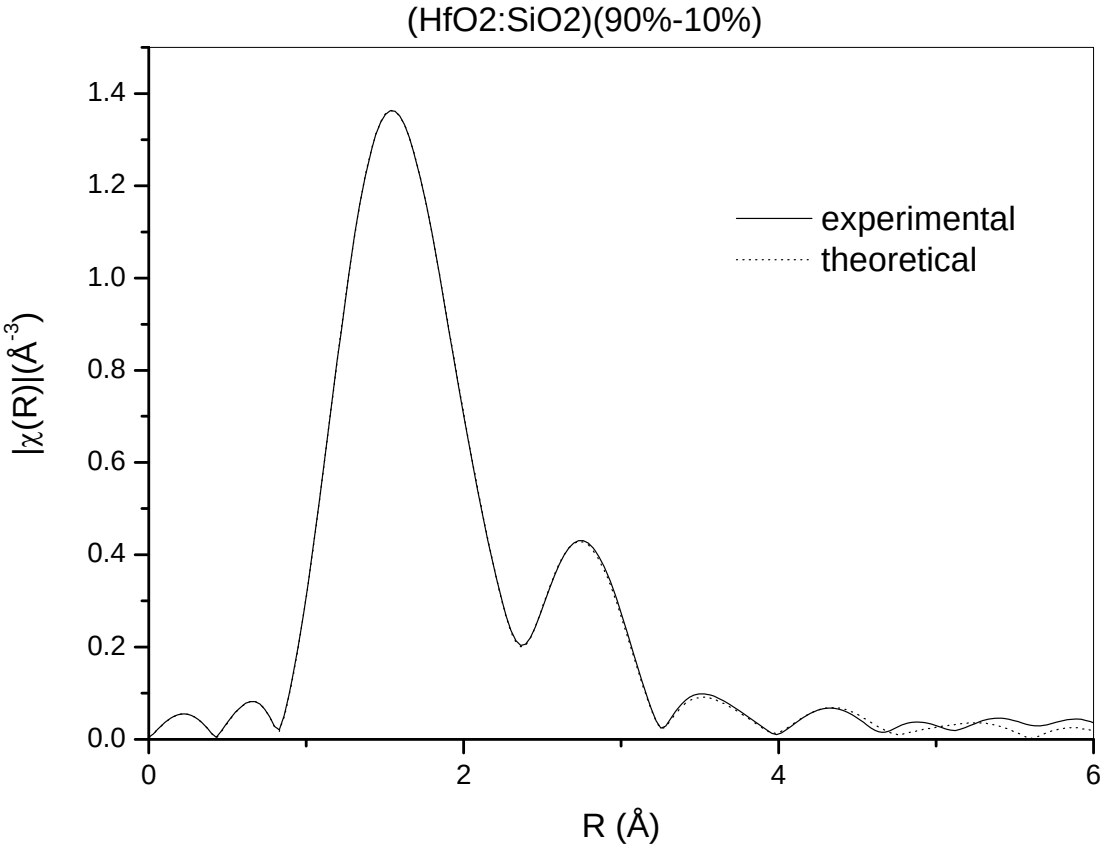

Fig.13: Fitting of FT spectrum in *R*-space with the theoretical spectrum corresponding to composite thin film having (HfO_2:SiO_2) composition of (90%:10%) and amorphous structure

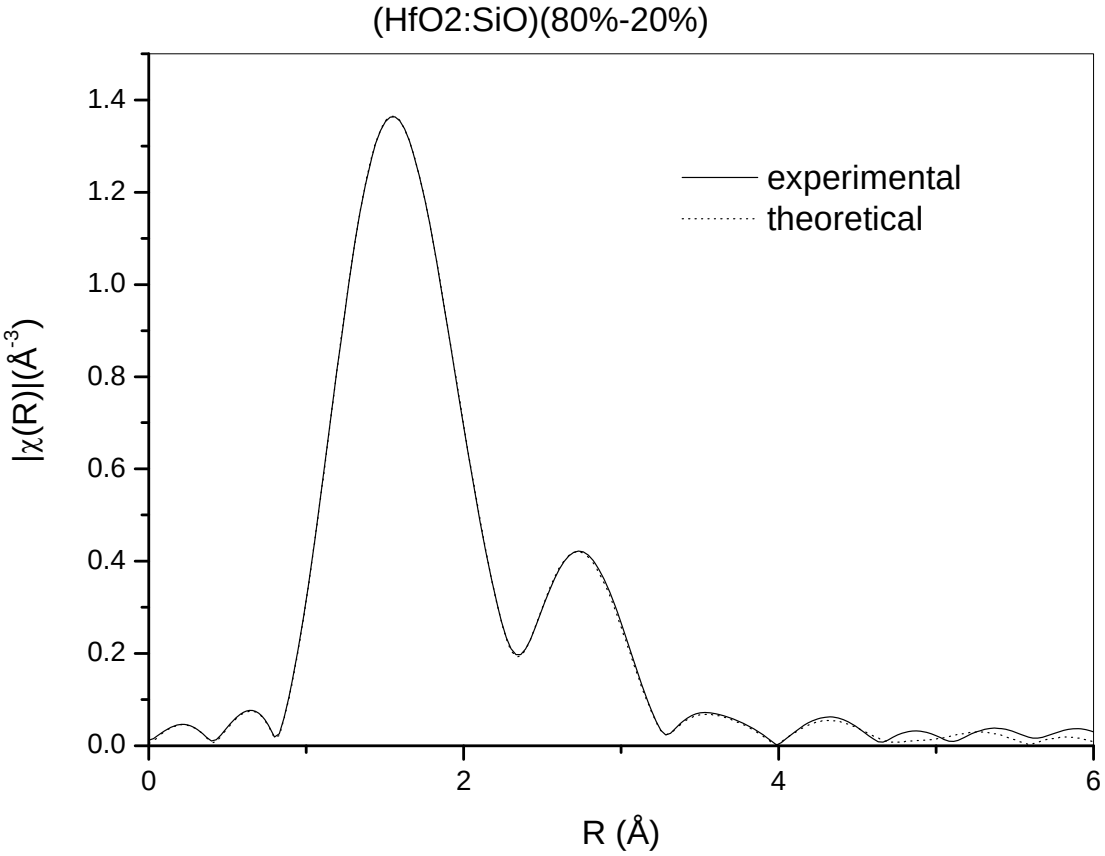

Fig.14: Fitting of FT spectrum in *R*-space with the theoretical spectrum corresponding to composite thin film having (HfO_2:SiO_2) composition of (80%:20%) and amorphous structure

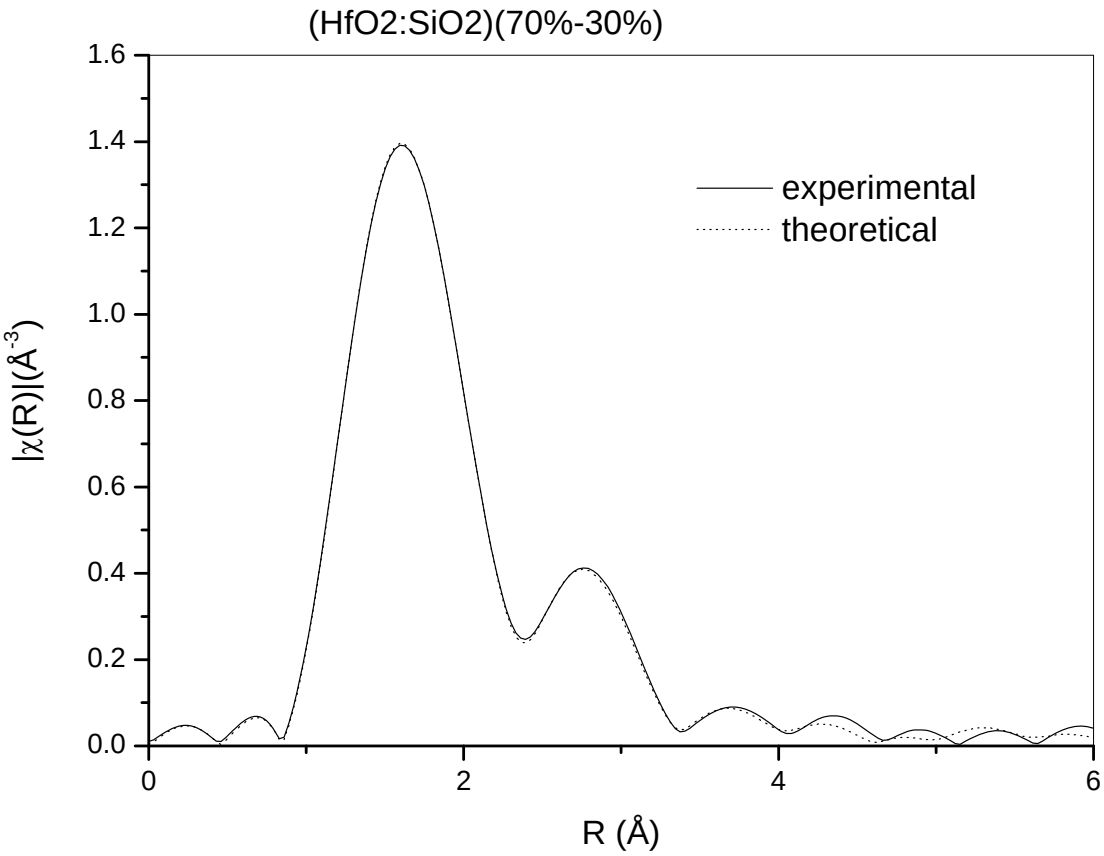

Fig.15: Fitting of FT spectrum in *R*-space with the theoretical spectrum corresponding to composite thin film having (HfO_2:SiO_2) composition of (70%:30%) and amorphous structure

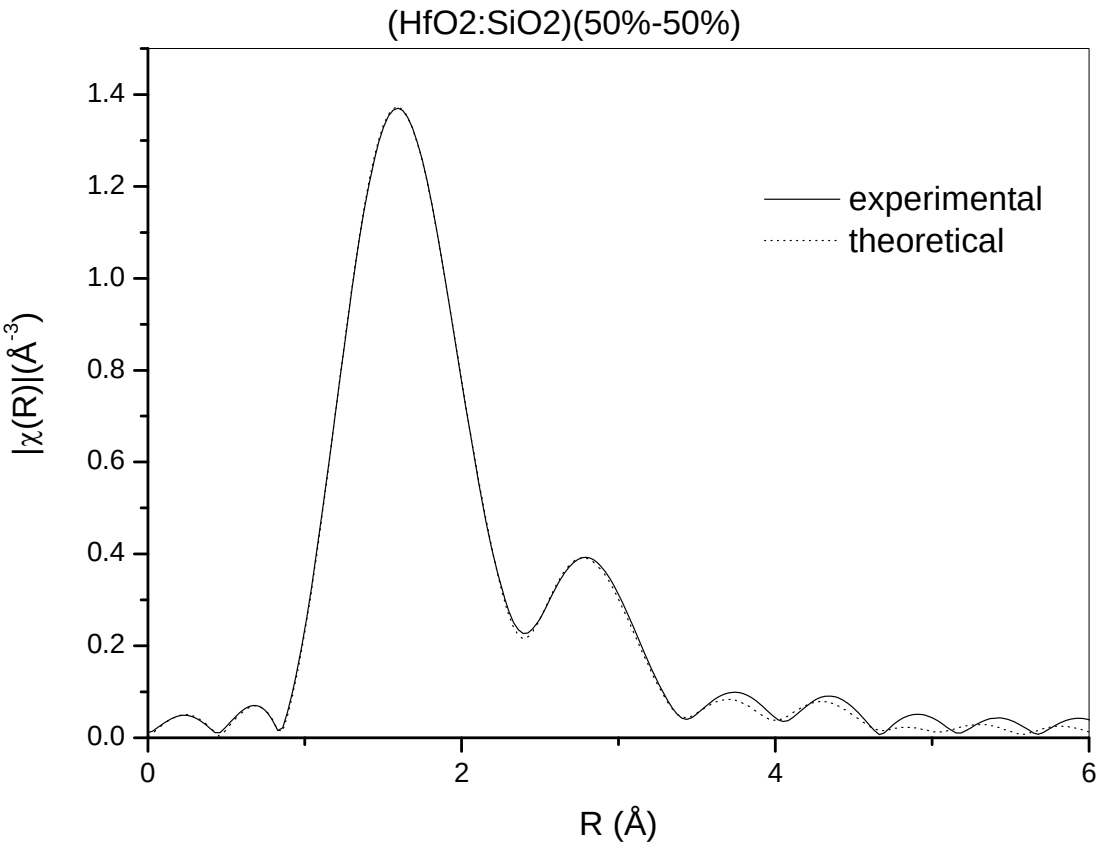

Fig.16: Fitting of FT spectrum in *R*-space with the theoretical spectrum corresponding to composite thin film having (HfO_2:SiO_2) composition of (50%:50%) and amorphous structure

Table 1

Structural parameters of the first (Hf-O), second (Hf-Hf) and third (Hf-Hf) coordination shells around hafnium in the thin film samples of HfO_2 and ($HfO_2 – SiO_2$) as obtained from EXAFS data modeling

Sample		HfO_2 (100%)	($HfO_2 – SiO_2$) (90% - 10%)	($HfO_2 – SiO_2$) (80% - 20%)	($HfO_2 – SiO_2$) (70% - 30%)	($HfO_2 – SiO_2$) (50% - 50%)
First coordination shell (Hf-O)	N (atoms)	7	7	7	6	6
	R(Å)	2.189	2.146	2.172	2.181	2.190
	σ^2(Å^2)	0.0317	0.0052	0.0039	0.0113	0.0252
Second coordination shell (Hf-Hf)	N (atoms)	7	7	7	6	5
	R(Å)	3.448	3.405	3.431	3.441	3.439
	σ^2(Å^2)	0.0317	0.0052	0.0039	0.0113	0.0252
Third coordination shell (Hf-Hf)	N (atoms)	6				
	R(Å)	3.804				
	σ^2(Å^2)	0.0174				